QED tenth-order contribution to the electron anomalous magnetic moment and a new value of the fine-structure constant

Fundamental Constants Meeting 2015
February 3, 2015
Eltville, Germany

Makiko Nio (RIKEN, Japan)

On behalf of the collaboration with
Toichiro Kinoshita (Cornell U, UMASS at Amherst),
Tatsumi Aoyama and Masashi Hayakawa (Nagoya U),
and K. Asano and N. Watanabe (Nagoya U)

new calculation of QED electron *g-2* & new value of *α*

AHKN(T. Aoyama, M. Hayakawa, T. Kinoshita, and M. Nio)

arXiv:1412.8284 to appear in Physical Review D in Feb. 2015.

updated and more precise values of the 8th- & 10th- order terms

D. Hanneke, S. Fogwell, and G. Gabrielse, PRL100, 120801 (2008)

This leads to a new value of the fine structure constant:

$$\alpha^{-1}(a_e : \mathrm{HV08}\ \&\ \mathrm{QED14}) = 137.035\ 999\ 1570\ \boxed{(29)(27)}(18)(331)\ \ [0.25\mathrm{ppb}]$$

$$\alpha^{-1}(a_e : \mathrm{HV08}\ \&\ \mathrm{QED12}) = 137.035\ 999\ 1727\ \boxed{(68)(46)}(19)(331)\ \ [0.25\mathrm{ppb}]$$

QED 8th, 10th , Weak&Hadron, Experiment

QED 8th-order term: (68) → (29), factor 2.3 improvement

10th-order term: (46) → (27), factor 1.7 improvement

Shift 157 is larger than the combined uncertainties of QED terms

⇨ Need explanation for the new QED results

Plan of talk

How accurate are the QED 8th and 10th-order terms?

0. *g-2* in QED, perturbation theory for *g-2*

1. Confirmation of part of the QED calculation by other groups
   - 8th-order diagrams including fermion loops
   - 10th-order diagrams, Set I, 208 Feynman vertex diagrams

2. Analytic work of our QED *g-2* calculation
   - automation of writing the integrands
   - identification of UV and IR subtraction terms

3. Numerical work of our QED *g-2* calculation
   - mapping from 14 Feynman parameters to 13 dim. cube
   - quadruple precision calculation w/ a double-double precision library

4. How far can we go ahead in precision of the QED calculation?

Anomalous magnetic moment(*g-2*) in QED

The standard-model contribution to the electron anomalous magnetic moment:

$$a_e \equiv (g-2)/2$$

$$a_e = a_e(\mathrm{QED}) + a_e(\mathrm{hadronic}) + a_e(\mathrm{electroweak})$$

a_e(QED) accounts for 99.999 999 8 % of a_e

a_e(QED) arises from contributions of

virtual photons and leptons

Perturbation theory of QED can well describe *g-2*:

$$a_e(\mathrm{QED}) = \frac{\alpha}{\pi} a_e^{(2)} + \left(\frac{\alpha}{\pi}\right)^2 a_e^{(4)} + \left(\frac{\alpha}{\pi}\right)^3 a_e^{(6)} + \left(\frac{\alpha}{\pi}\right)^4 a_e^{(8)} + \cdots$$

$$a_e^{(2n)} = A_1^{(2n)} + A_2^{(2n)}(m_e/m_\mu) + A_2^{(2n)}(m_e/m_\tau) + A_3^{(2n)}(m_e/m_\mu, m_e/m_\tau)$$

QED non-perturbative effect on vp function

Recent discussion on positronium contribution to *g-2*: vacuum-polarization(vp) function consisting of infinitely many Coulomb photons

G. Mishima, arXiv:1311.7109
M. Fael and M. Passera, PRD 90, 056004 (2014)

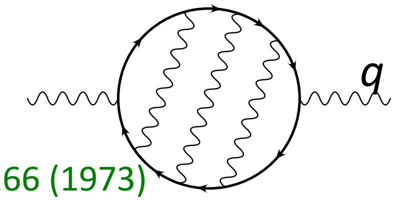

When $q^2 \sim 4 m_e^2$,

M. A. Braun, Zh. Eksp. Teor. Fiz. 54, 1220 (1968)
R. Barbieri, P. Christillin, and E. Remiddi, PRA 8, 2266 (1973)

need to sum up all Coulomb photon exchange diagrams

$$\Pi(\text{non-perturvative})(q^2) = \Pi(\text{bound state}) + \Pi(\text{Coulomb scattering}) - \Pi(\text{overlap with perturbative calculation})$$

q^2 dependence of bound state and Coulomb scattering terms is

$\boxed{\dfrac{\alpha m_e}{\sqrt{q^2 - 4m_e^2}}}$, it cannot be expanded if $q^2 \sim 4 m_e^2$

The overlapping term is obtained from the sum of bound. + scatt. taking the limit $q^2 \to -\infty$ and expanding it in power series of α.

QED non-perturbative VP contribute to *g-2*?

No.

K. Melnikov, A. Vainshtein, and M. Voloshin, Phys. Rev. D 90, 017301 (2014)
M. I. Eides, Phys. Rev. D 90, 057301 (2014) , M. Fael and M. Passera, PRD 90, 056004(2014)

No non-perturbative effect on *g-2* exists in any power of *α.*

VP function effect on *g-2* through a virtual photon:

$$M_{2,\mathrm{vp}} = -\int_0^1 dy(1-y)\Pi(-\frac{y^2}{1-y})$$

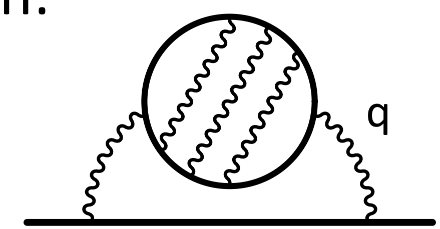

$q^2 = - y^2 /(1-y) < 0$ as a consequence of

Wick rotation of a loop momentum q^2

For $q^2 < 0$, $\dfrac{\alpha m_e}{\sqrt{q^2 - 4m_e^2}}$ is a small parameter.

Both bound. and scatt. terms are expandable in $\dfrac{\alpha m_e}{\sqrt{q^2 - 4m_e^2}}$.

This is nothing but the overlapping term.

Trivially they cancel out each other.

Thus, the non-perturbative vp cannot contribute to *g-2*.

QED perturbation 2,4, and 6th orders

2,4, and 6th-order terms both mass-dependent and mass-independent terms are well established

mass-independent terms:

J. S. Schwinger, Phys. Rev. 73, 416 (1948)
A. Petermann, Helv. Phys. Acta 30, 407 (1957)
C. M. Sommerfield, Ann. Phys. (N.Y.) 5, 26 (1958)
S. Laporta and E. Remiddi, Phys. Lett. B379, 283 (1996)

$$A_1^{(2)} = 0.5$$

$$A_1^{(4)} = -0.328\ 478\ 965\ 579\ 193\cdots$$

$$A_1^{(6)} = 1.181\ 241\ 456\cdots$$

mass-dependent terms:

H. H. Elend, Phys. Lett. 20, 682 (1966)
M. A. Samuel and G.-w. Li,
PRD 44, 3935 (1991), 48, 1879(E) (1993)
G. Li, R. Mendel, and M. A. Samuel,
PRD 47, 1723 (1993)

$$A_2^{(4)}(m_e/m_\mu) = 5.197\ 386\ 67\ (26) \times 10^{-7}$$

$$A_2^{(4)}(m_e/m_\tau) = 1.837\ 98\ (34) \times 10^{-9}$$

$$A_2^{(6)}(m_e/m_\mu) = -7.373\ 941\ 55\ (27) \times 10^{-6}$$

$$A_2^{(6)}(m_e/m_\tau) = -6.5830\ (11) \times 10^{-8}$$

$$A_3^{(6)}(m_e/m_\mu, m_e/m_\tau) = 1.909\ (1) \times 10^{-13}$$

S. Laporta and E. Remiddi, PLB301, 440 (1993)
S. Laporta, Nuovo Cim. A106, 675 (1993)
M. Passera, Phys. Rev. D 75, 013002 (2007)

Uncertainties come from the lepton mass-ratios only.

QED 8th-order terms

New 8th-order terms

AHKN, arXiv:1412.8284

$$\boxed{A_1^{(8)} = -1.912\ 98\ (84)}$$

consistent

Improvement in numerical integration

8th-order terms in 2012

AHKN, PRL109(2012) 111807

$$A_1^{(8)} = -1.9106\ (20)$$

A. Kurz, T. Liu, P. Marquard, and M. Steinhauser, Nucl. Phys. B879, 1 (2014)

$$A_2^{(8)}(m_e/m_\mu) = 9.161\ 970\ 703\ (373) \times 10^{-4}$$

$$A_2^{(8)}(m_e/m_\tau) = 7.429\ 24\ (118) \times 10^{-6}$$

$$A_3^{(8)}(m_e/m_\mu, m_e/m_\tau) = 7.4687\ (28) \times 10^{-7}$$

Heavy lepton-mass expansion, analytic results

AHKN, PRL109(2012) 111807

$$A_2^{(8)}(m_e/m_\mu) = 9.222\ (66) \times 10^{-4}$$

$$A_2^{(8)}(m_e/m_\tau) = 8.24\ (12) \times 10^{-6}$$

$$A_2^{(8)}(m_e/m_\tau) = 7.38\ (12) \times 10^{-6}$$

$$A_3^{(8)}(m_e/m_\mu, m_e/m_\tau) = 7.465\ (18) \times 10^{-7}$$

Group I(d) contribution to $A_2^{(8)}(m_e/m_\tau)$ in AHKN, PRL109 is a typo.

wrong → right

0.8744(1) x10^{-6} → 0.008 744 (1) x 10^{-6}

8^{th}-order independent check

891 vertex Feynman diagrams divided into 13 gauge-invariant groups:

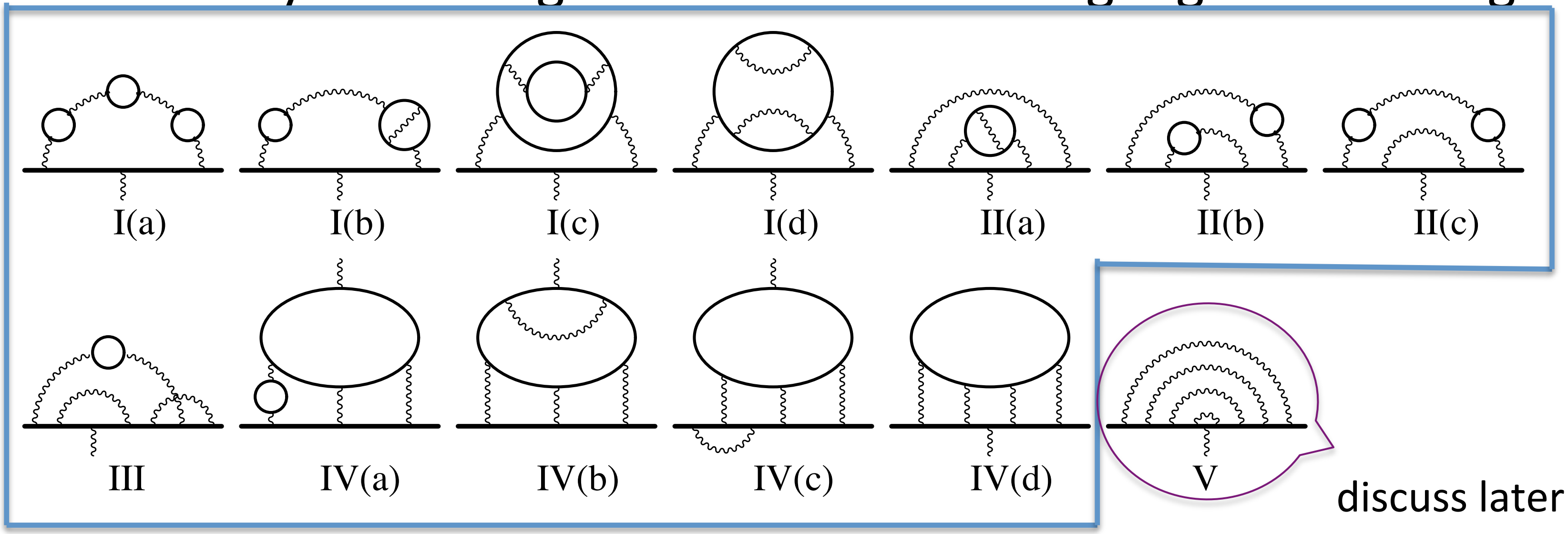

373 diagrams, 12 groups, contribute to

the mass-dependent terms A_2 and/or A_3 .

With correction of IV(d) in 2003 Kinoshita and Nio, PRL90(2003)021803,

our numerical and their analytic calculations are in good agreement.

Our numerical approach to 12 groups is

correct even for the mass-independent term A_1

because we need only to replace $r=m_\mu/m_e$ =206.76…. by r=1.

QED 10th-order terms

New 10th-order terms

AHKN, arXiv:1412.8284

$$\boxed{A_1^{(10)} = 7.795\ (336)}$$

10th-order terms in 2012

AHKN, PRL109(2012) 111807

$$A_1^{(10)} = 9.16\ (58)$$

Shift −1.37 is much larger than the uncertainties, 0.34 and 0.58

- No analytic incorrectness has been found in the whole 10th-order calculation.
- The shift comes purely from the numerical integrations.
- The diagrams concerned with are 6354 Feynman diagrams

of Set V involving no fermion loop, only photonic corrections.

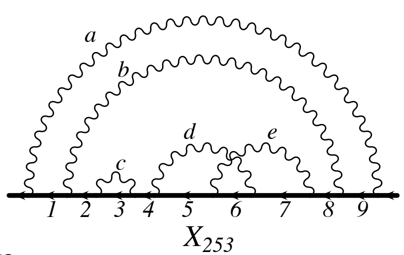

discuss later

This is the cause of the shift in α determined from the electron *g-2*.

Muon contribution has not been changed from the 2012 value:

$$A_2^{(10)}(m_e/m_\mu) = -0.003\ 82\ (39)$$

tau-lepton contribution is too small.

10^{th}-order Feynman diagrams

12,672 vertex Feynman diagrams can be divided into 32 gauge-invariant sets:

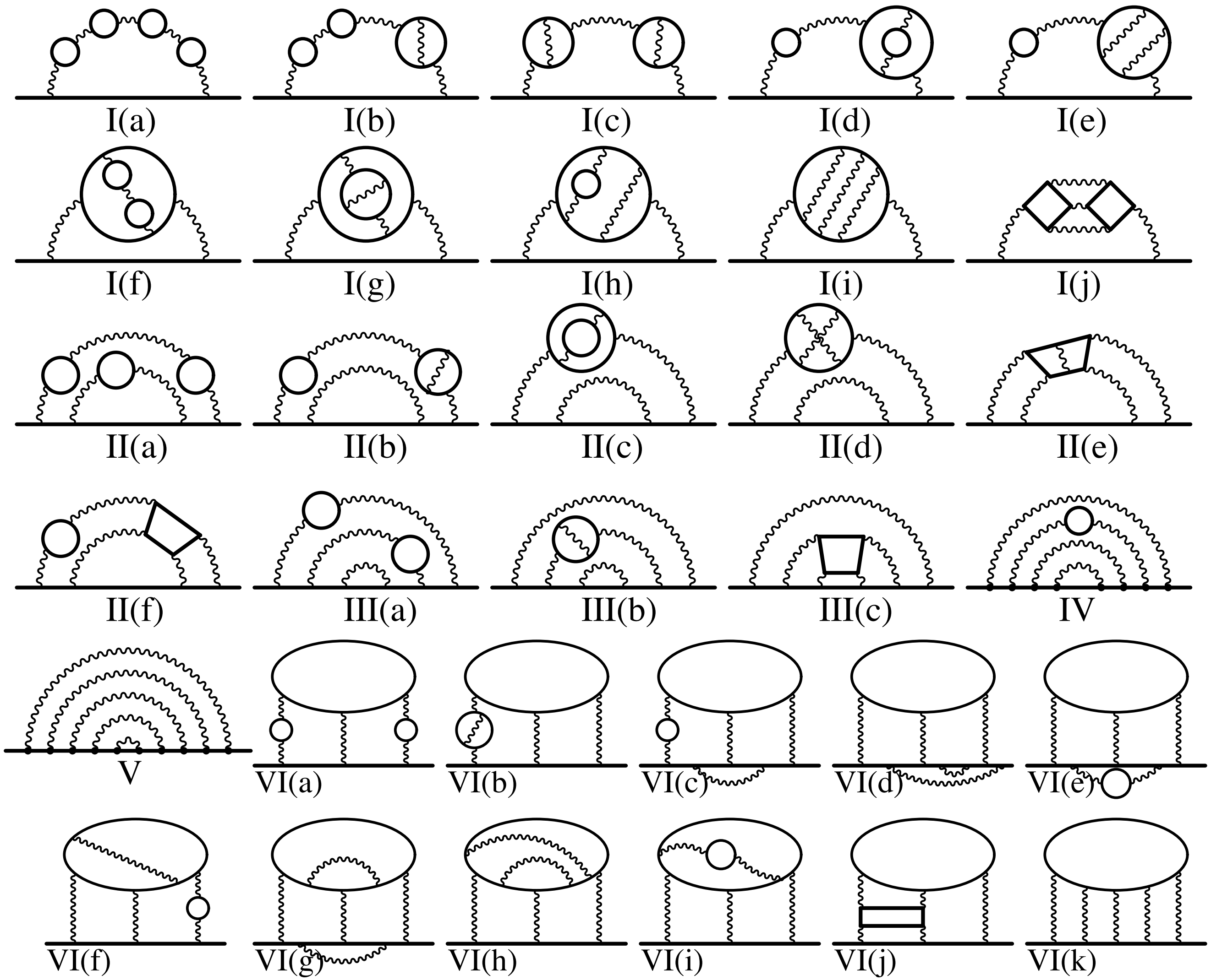

Independent check of 10th-order Set I

Recently, Set I, 208 diagrams are (semi-)analytically calculated for both electron and muon *g-2*, and their mass-dependent and mass-independent terms: P. A. Baikov, A. Maier, and P. Marquard, Nucl. Phys. B877, 647 (2013)

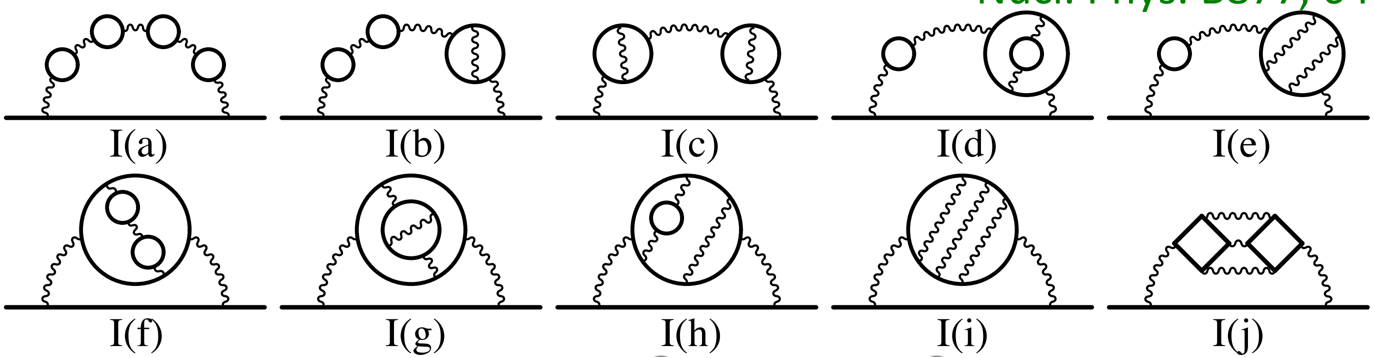

Table 3 from Baikov et al.

Contributions to the mass-independent term $A_1^{(10)}$

AHKN, PRL109(2012) 111807

	Baikov et al.	AHKN, PRL 2012
I(a)	0.000 471	0.000 470 94 (6)
I(b)	0.007 010	0.007 010 8 (7)
I(c)	0.023 467	0.023 468 (2)
I(d)+I(e)	0.014 094	0.014 098 (5)(4)
I(e)	0.010 291	0.010 296 (4)
I(f)+I(g)+I(h)	0.03785^{+5}_{-3}	0.037 833 (20)(6)(13)
I(i)	$0.017\ 21^{+8}_{-23}$	0.017 47 (11) $\to$ 0.017 324 (12)
I(j)	$0.000\ 420^{+31}_{-16}$	0.000 397 5 (18)

theoretical value of the electron *g*-2

Hadronic and weak corrections are small but not negligible:

- $a_e(\mathrm{hadronic}) = (1.866(10)(5) - 0.2234(12)(7) + 0.035(10)) \times 10^{-12}$
- $a_e(\mathrm{electroweak}) = 0.0297\ (5) \times 10^{-12}$

D. Nomura and T. Teubner, NPB867, 236 (2013)
J. Prades, E. de Rafael, and A. Vainshtein, in 'Lepton Dipole Moments', (2009), pp. 303.
M. Knecht, S. Peris, M. Perrottet, and E. de Rafael, JHEP 11, 003 (2002).

K. Fujikawa, B. W. Lee, and A. I. Sanda, PRD 6, 2923 (1972).
A. Czarnecki, B. Krause, and W. J. Marciano, PRL. 76, 3267 (1996).
A. Czarnecki, W. J. Marciano, and A. Vainshtein, PRD 67, 073006 (2003), 73, 119901(E) (2006).

Input values for $a_e(\mathrm{QED})$:

α is from the *h/m*$_{Rb}$ measurement

$$\alpha^{-1}(\mathrm{Rb10}) = 137.035\ 999\ 049\ (90)\ [0.66\mathrm{ppb}]$$

R. Bouchendira, P. Cladé, S. Guellati-Khélifa, F. Nez, and F. Biraben, PRL106, 080801 (2011)

$$m_e/m_\mu = 4.836\ 331\ 66\ (12) \times 10^{-3}$$

$$m_e/m_\tau = 2.875\ 92\ (26) \times 10^{-4}$$

P. J. Mohr, B. N. Taylor, and D. B. Newell, Rev. Mod. Phys. 84, 1527 (2012)

$$a_e(\mathrm{theory}) = 1\ 159\ 652\ 181.643(25)(23)(16)(763) \times 10^{-12}$$

8th, 10th, weak&hadron, α(Rb10)

D. Hanneke, S. Fogwell, and G. Gabrielse, PRL100, 120801 (2008)

$$a_e(\mathrm{HV08}) = 1\ 159\ 652\ 180.73(28) \times 10^{-12}\ [0.24\mathrm{ppb}]$$

$$a_e(\mathrm{HV08}) - a_e(\mathrm{theory}) = -0.91\ (0.82) \times 10^{-12}$$

Diagrams w/o closed lepton loops

The uncertainties of $A_1^{(8)}$ and $A_1^{(10)}$ entirely come from Group V and Set V, respectively.

Let us focus on Group V and Set V.

8^{th}-order Group V: 518 of 819 vertex Feynman diagrams

10^{th}-order Set V: 6,354 of 12,672 vertex Feynman diagrams

Summing up the vertex diagrams w/ similar photon corrections:

$$\boxed{\Lambda^{\nu}(p,q) \simeq -q_{\mu}\left[\frac{\partial\Lambda_{\mu}(p,q)}{\partial q_{\nu}}\right]_{q=0} - \frac{\partial\Sigma(p)}{\partial p_{\nu}}}$$

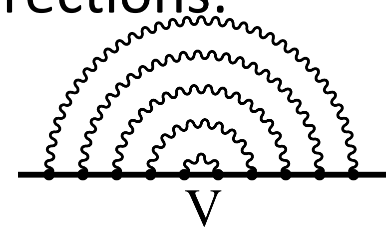

Thanks for the gauge symmetry and Ward-Takahashi identity.

Time reversal symmetry

8^{th}-order Group V: 518/7=74 → 47 independent integrals

10^{th}-order Set V: 6,354/9=706 → 389 independent integrals

represented by self-energy like diagrams

47 self-energy like diagrams of 8th-order Group V

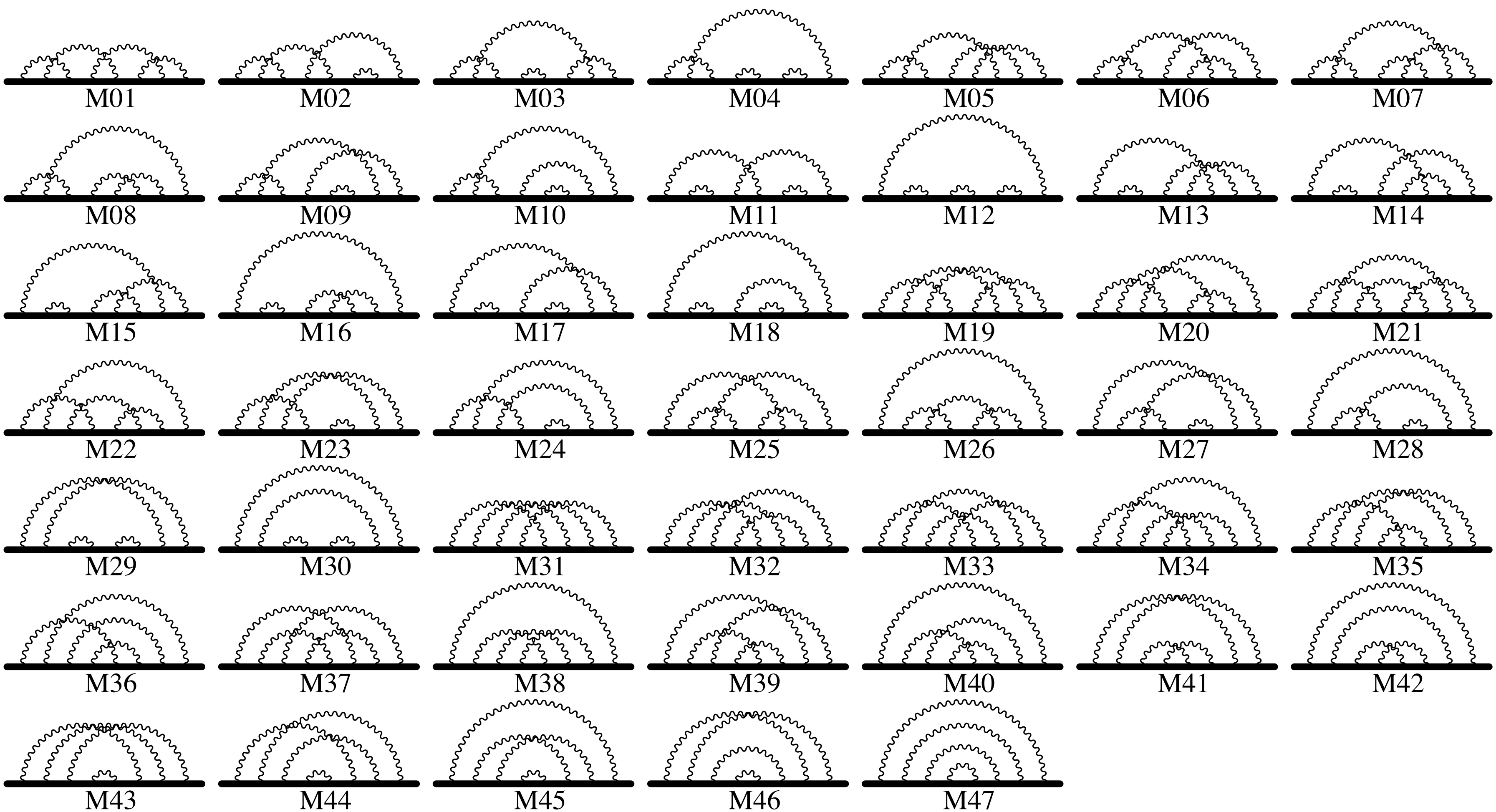

389 self-energy like diagrams of 10th-order Set V

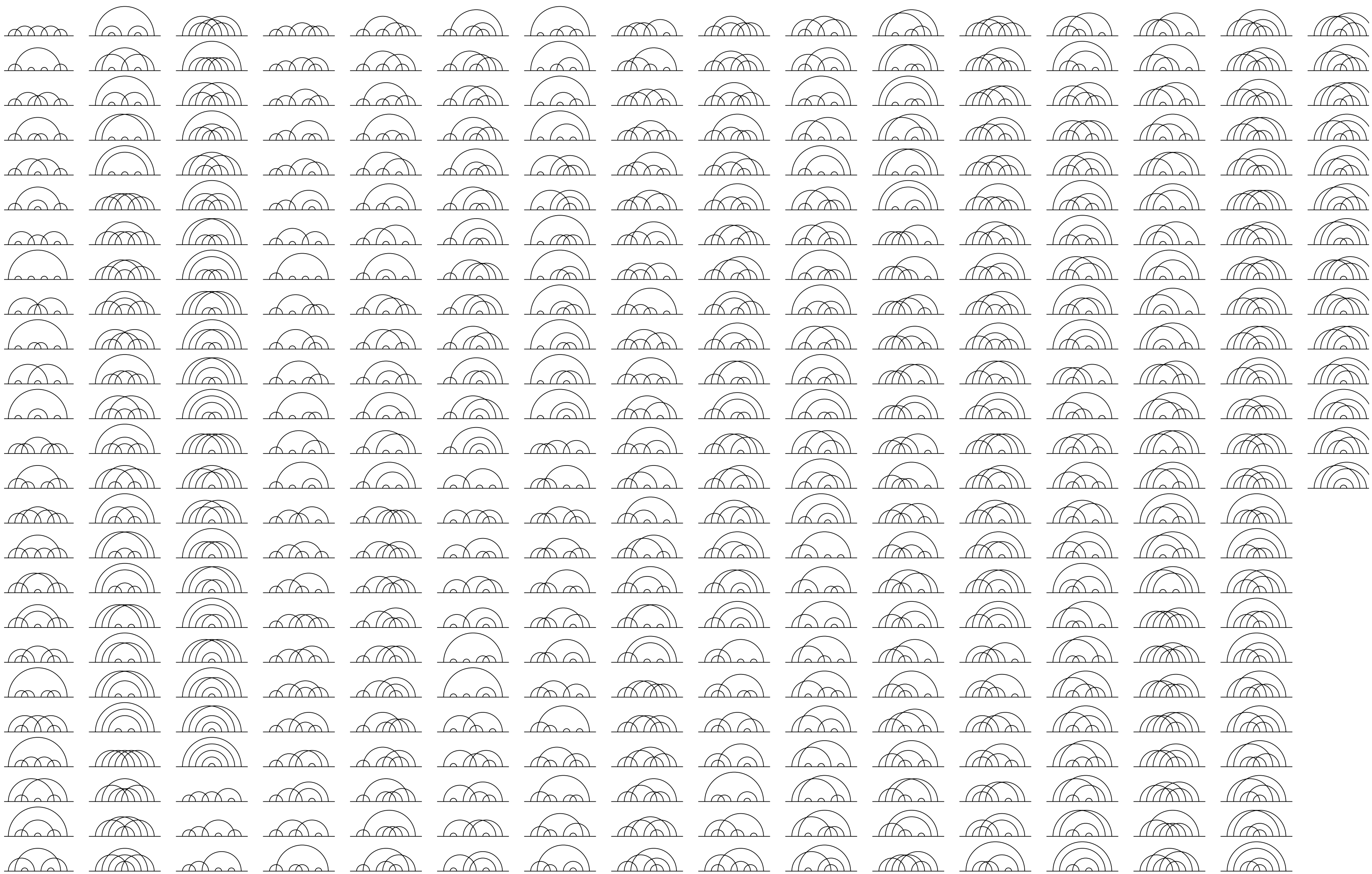

Automatic calculation w/ gencodeN

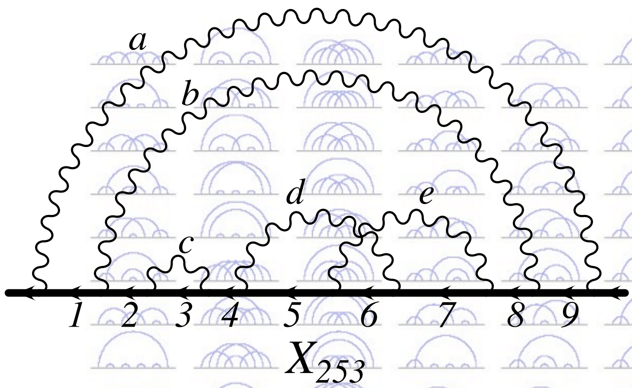

gencodeN can handle
a diagram w/o fermion loops
at any order of the perturbation theory

automation

About 72,000 lines

1. Bare Amplitude M(X253)
2. UV subtraction terms
   $M(\mathrm{X253})^{\mathrm{R}} = M(\mathrm{X253}) - (23\ \mathrm{UV\ terms})$
3. IR subtraction terms
   $\Delta M(\mathrm{X253}) = M(\mathrm{X253})^{\mathrm{R}} - (91\ \mathrm{IR\ terms})$

When they are numerically integrated by VEAGS,
quadruple precision for real numbers is used.

超並列 PC クラスタ RIKEN's RICC 2009- now
Peak 96Tflops
RIKEN's RSCC 2004-2009
Peak 12Tflops

Test of gencodeN w/ 8th-order Group V

8th-order Group V, 47 integrals + residual renormalization

- 1st try w/ human effort T. Kinoshita, W. B. Lindquist, PRD 42 (1990) 635

  UV & IR terms are identified using power counting rules

- 2nd try w/ gencodeN AHKN, PRL99(2007)110406

  UV terms are same. IR terms are different in finite amount

47 integrals of Group V are compared:

1st calculation ?=? 2nd calculation + finite term due to IR difference

separately calculated

- All 47 integrals are **OK**. AHKN, PRD77(2008)053012

M16 & M18 of the 1st try should receive a finite correction.

inconsistency between the IR subtraction terms of their integrands and those of the residual renormalization term.

Fine-structure constant α: a_e and Rb

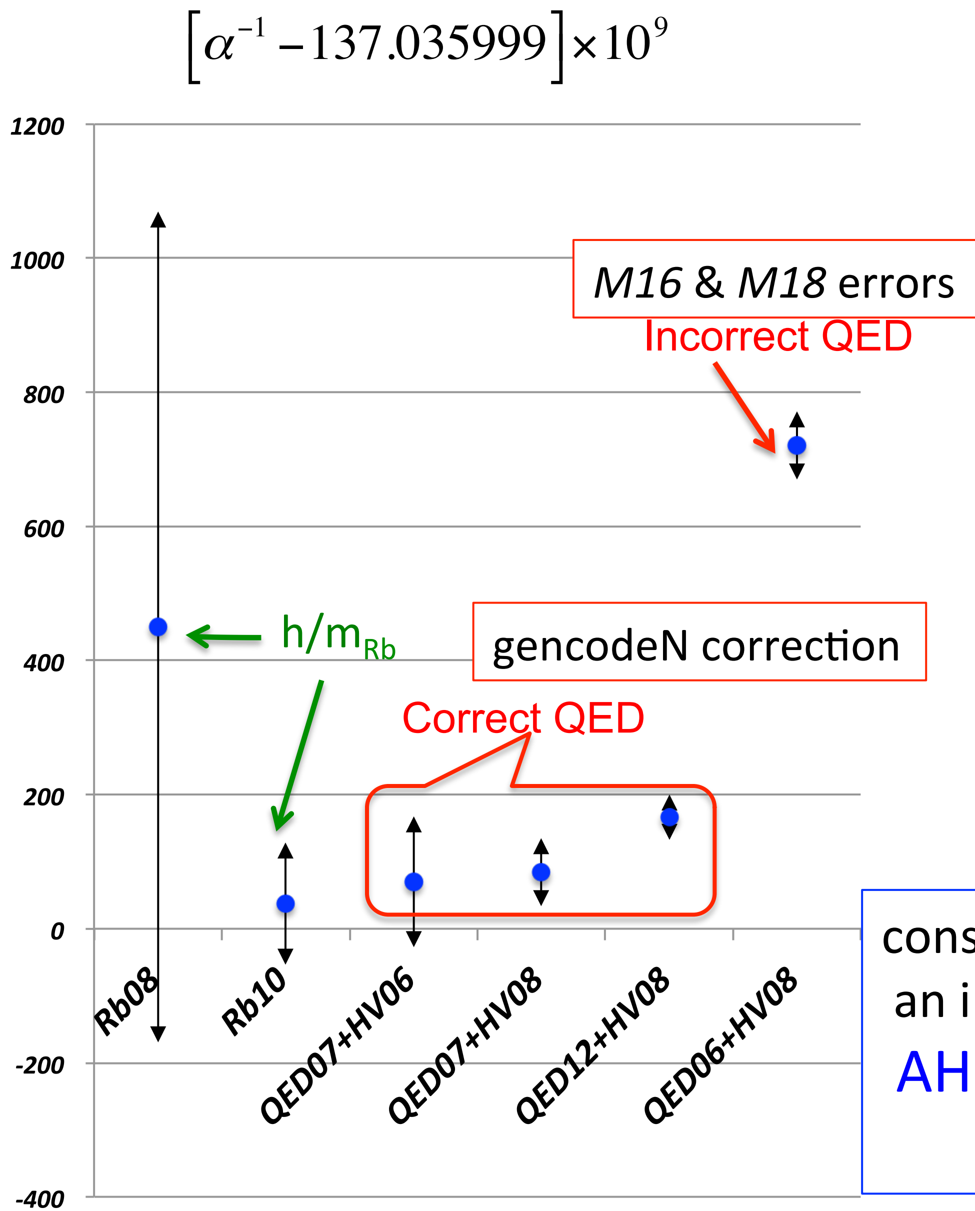

$$a_e(expt.) = a_e(theory;\alpha)$$

$$\alpha^2 = \frac{2R_\infty}{c}\frac{m_{Rb}}{m_e}\frac{h}{m_{Rb}}$$

R_∞	Rydberg constant
c	Speed of light, exact
m_{Rb}	Mass of Rb atom
m_e	Mass of electron
h	Planck constant

consistency between $\alpha(a_e)$ and α(Rb10) is an indirect proof that

AHKN's 2nd try w/ gencodeN is on the right track.

gencodeN for 10th-order Set V

389 numerically calculable integrands are made by gencodeN:

$\Delta M(X\ldots) = M(X\ldots;\text{ bare term}) - (\text{UV subtraction}) - (\text{IR subtraction})$

Does gencodeN correctly work even for the 10th-order Set V?

1. Bare terms **OK✔**

   trivial extension from the lower-order

2. UV subtraction terms by K-operation **OK✔**

   UV divergence occurs from only vertex and self-energy subdiagrams.

   if UV divergence is left in ΔM, numerical integration immediately breaks down.

3. IR subtraction terms by R-subtraction and I-operation not **OK**

   numerical integration cannot distinguish IR divergence from

   fluctuation of the integral due to small statistics.

We analytically identified what the missing IR subtraction terms are.

R-subtraction in gencodeN

Two kinds of IR divergence mechanism

1. R-subtraction: residual mass-renormalization

our UV renormalization by K-operation for the mass-renormalization subtracts part of the mass-renormalization term

determined by K-operation

standard mass-renormalization $-dm4a \times M6c(4^*)$

UV renormalization by K-operation $-\boxed{dm4a^{UV}} \times M6c(4^*)$

R-subtraction $-dm4a^{R} \times M6c(4^*)$,

$$\text{where } dm4a = dm4a^{UV} + dm4a^{R}$$

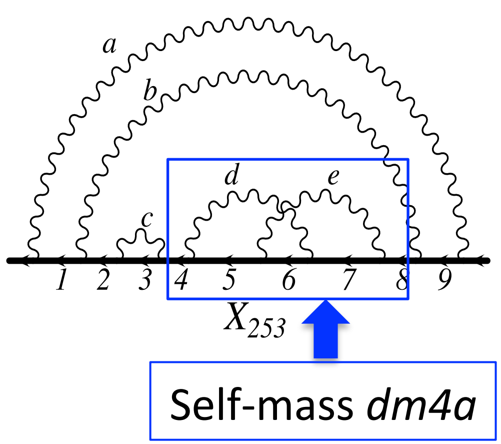

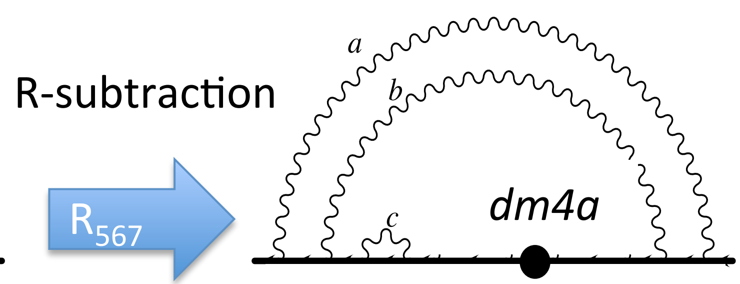

Residual diagram *M6c(4*)* has one more electron line than *M6c* because of a mass insertion.

the IR divergence comes from the magnetic moment *M6c(4*)*

I-operations in gencodeN

2. I-operation:

a lower-order magnetic moment

× a vertex renormalization constant

I-operation $\quad - L6c(4)^{R} \times M4a,$

where $\quad L6c(4)^{R} = L6c(4) - \boxed{L6c(4)^{UV}}$ ← determined by K-operation

$- \boxed{\text{all kinds of uv divergence in } (L6c(4) - L6c(4)^{UV})}$

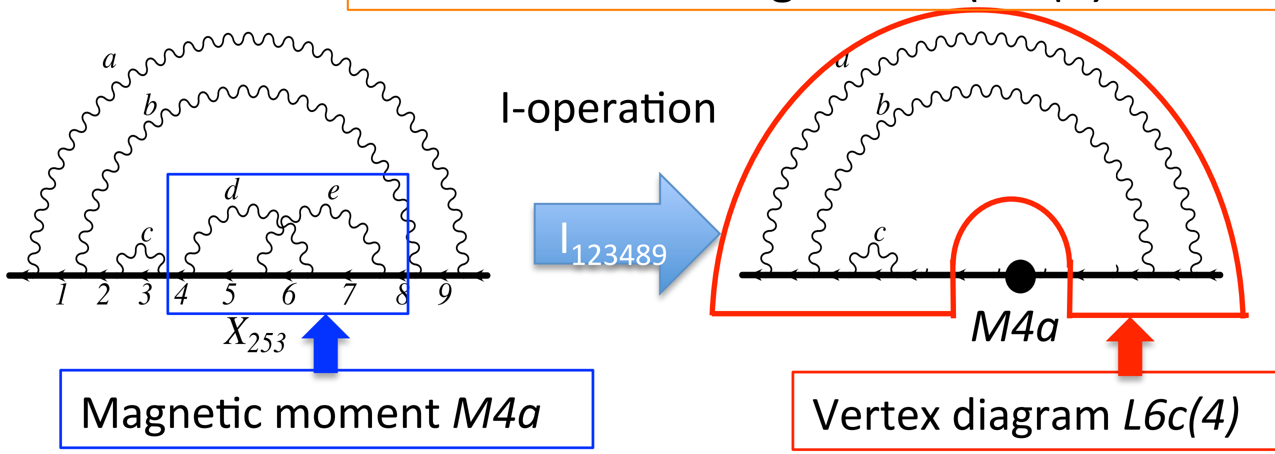

the IR divergence comes form the vertex renorm. constant $L6c(4)^{R}$

Nested I and R-subtractions in gencode N

One of nested IR singularities in X253, I_{19} I_{248} R_{567}

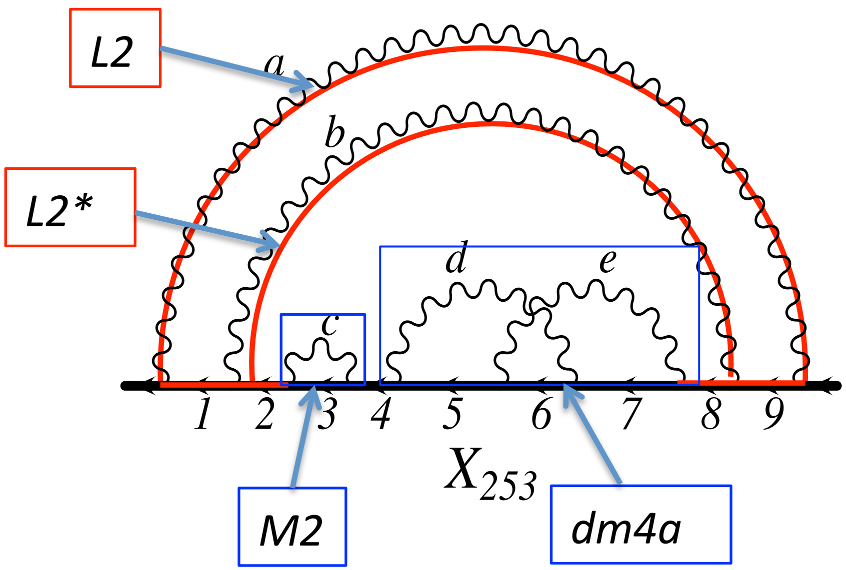

{3c} magnetic moment *M2*

{567de} self-mass *dm4a*

{19a} vertex *L2*

{28b} vertex *L2**

The IR subtraction term should be $-L2^{R} \times L2^{*} \times dm4a^{R} \times M2.$

But, the rule in gencodeN uses $L2^{*R}$ instead. Similar to $L2^{R}$.

$$L2 = \underbrace{L2^{UV}}_{\text{UV term}} + \underbrace{L2^{R}}_{\text{IR term}},$$

$$L2^{*} = \underbrace{\Delta L2^{*}}_{\text{finite term}} + \underbrace{L2^{*R}}_{\text{IR term}}$$

Code modification for X253 and X256

So, we should make the IR subtraction terms by hand

$-L2^{R} \times \Delta L2^{*} \times dm4a^{R} \times M2$ *for* X253

$-L2^{R} \times \Delta L2^{*} \times dm4b^{R} \times M2$ *for* X256

There are only two diagrams at the 10^{th} order which require the code modification.

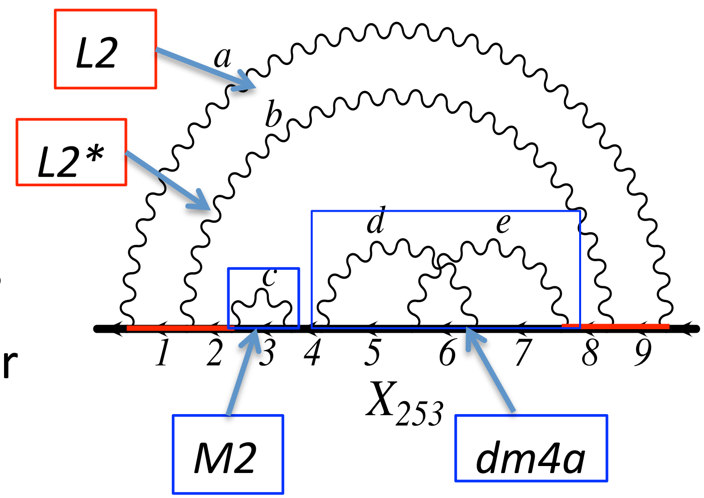

Necessary conditions:

- a rainbow structure, at least 1+1 powers of α
- a self-mass inside the rainbow, at least 2 powers

∵ UV K-operation entirely subtracts the 2^{nd}-order self-mass *dm2.*

- a self-energy diagram which provides a magnetic moment should exists. At least 1 power.

The 389 integrals of Set V are ready to go to numerical evaluation.

These IR terms were already included in our 2012 result.

Residual renormalization

The sum of our 389 integrals is not the physical contribution to *g-2*.
We adapt the standard-on-shell renormalization scheme to ensure

- the coupling constant α is the one measured by experiments.
- the electron masse m_e is the one measured by experiments.

$$a_e \overset{\text{def.}}{=} M(\text{bare}) - (\text{standard on-shell renormalization})$$

$$= [\, M(\text{bare}) - (\text{UV subtraction}) - (\text{IR subtraction})\,]$$

Finite integral ΔM made by gencodeN and to be numerically evaluated

$$+ [\, -(\text{standard renorm.}) + (\text{UV sub.}) + (\text{IR sub.})\,]$$

Finite residual renormalization

We need to know what the residual renormalization formula is
and what its numerical value is.

Derivation of the residual renorm.: direct sum

gencodeN knows what the UV and IR subtraction terms are.

Example: X253

- UV forests: 23

$K28$	$-dm16^{\mathrm{UV}}\ M2* - B16^{\mathrm{UV}}\ M2$
$K33$	$-dm2^{\mathrm{UV}}\ M42(2*) - B2^{\mathrm{UV}}\ M42$
$K56$	$-L2^{\mathrm{UV}}\ M30$
$K57$	$-dm4a^{\mathrm{UV}}\ M6b(2*) - B4a^{\mathrm{UV}}\ M6b$
$K67$	$-L2^{\mathrm{UV}}\ M30$
$K28\_33$	$+dm2^{\mathrm{UV}}\ dm6c(1*)^{\mathrm{UV}}\ M2* + B2^{\mathrm{UV}}\ dm6c1p^{\mathrm{UV}}\ M2* + B2^{\mathrm{UV}}\ B6c1p^{\mathrm{UV}}\ M2$
$K28\_56$	$+L2^{\mathrm{UV}}\ dm6a^{\mathrm{UV}}\ M2* + L2^{\mathrm{UV}}\ B6a^{\mathrm{UV}}\ M2$
$K28\_57$	$+dm4a^{\mathrm{UV}}\ dm4b(1*)^{\mathrm{UV}}\ M2* + B4a^{\mathrm{UV}}\ dm4b(1')^{\mathrm{UV}}\ M2* + B4a^{\mathrm{UV}}\ B4b(1')^{\mathrm{UV}}\ M2$
$K28\_67$	$+L2^{\mathrm{UV}}\ dm6a^{\mathrm{UV}}\ M2* + L2^{\mathrm{UV}}\ B6a^{\mathrm{UV}}\ M2$
$K33K56$	$+dm2^{\mathrm{UV}}\ L2^{\mathrm{UV}}\ M6b(2*) + B2^{\mathrm{UV}}\ L2^{\mathrm{UV}}\ M6b$

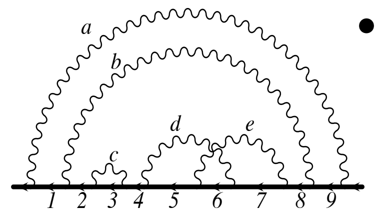

X_{253}

- IR annotated forests: 91

$R28$	$-dm16^{\mathrm{R}}\ M2*$
$I19$	$-L2^{\mathrm{R}}\ M16^{\mathrm{R}}$
$I12456789$	$-L422^{\mathrm{R}}\ M2$
$R57$	$-dm4a^{\mathrm{R}}\ M6b(2*)^{\mathrm{R}}$
$I123489$	$-L6b2^{\mathrm{R}}\ M4a^{\mathrm{R}}$
$I19I245678$	$+L6c1^{\mathrm{R}}\ L2^{\mathrm{R}}\ M2$
$K28RR57$	$+dm4a^{\mathrm{R}}\ dm4b(1*)^{\mathrm{R}}\ M2*$
$I19R57$	$+dm4a^{\mathrm{R}}\ L2^{\mathrm{R}}\ M4b(1*)^{\mathrm{R}}$
$I19I2348$	$+L4b1^{\mathrm{R}}\ L2^{\mathrm{R}}\ M4a^{\mathrm{R}}$
$I12489R57$	$+dm4a^{\mathrm{R}}\ L4b2(2*)^{\mathrm{R}}\ M2$

and others

Further decomposition of lower order terms:

eg. $M4a = 2\ L2^{\mathrm{UV}}\ M2 + \Delta M4a$, $M4b = dm2\ M2* + B2^{\mathrm{UV}} M2 + L2^{\mathrm{R}}\ M2 + \Delta M4b$

Sum up over 389 integrals of Set V, which requires

analytic sum over ~16,000 symbolic UV & IR terms.

Derivation of residual renom.: hand-waving

Consider a 8^{th}-order diagram *M8* w/ a 2^{nd}-order correction.

- 7 fermion lines → 2^{nd}-order self-energy *B2* can be inserted in 7 ways
- 8 vertices → 2^{nd}-order vertex *L2* can correct a vertex in 8 ways.
- Standard renormalization must have $\boxed{(7\, B2 + 8\, L2)\, M8}$,

  where *M8* is the sum of all 8^{th}-order bare magnetic moments.

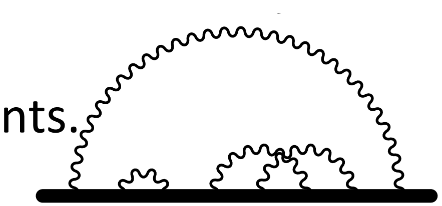

UV-subtraction term involving *M8*

- K-operation should yield the term $\boxed{(7\, B2^{UV} + 8\, L2^{UV})\, M8}$.

IR-subtraction term involving *M8*

- I-operation should yield the term $\boxed{L2^{R}\, M8}$

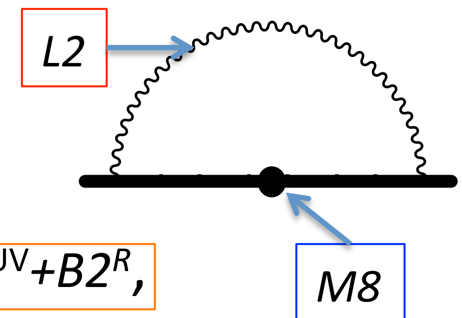

The residual renorm. term. Using $\boxed{L2 = L2^{uv} + L2^{R},\ B2 = B2^{UV} + B2^{R}}$,

$$\boxed{-(7\, B2 + 8\, L2)\, M8 + (7\, B2^{UV} + 8\, L2^{UV})\, M8 + L2^{R}\, M8 = -7\, (B2^{R} + L2^{R})\, M8}$$

Because of Ward-Takahashi identity $B2+L2=0$, the IR singularity in the sum $(B2^{R}+L2^{R})$ cancels out, and it is finite: $\boxed{\Delta LB2 = (B2^{R} + L2^{R})}$

We must have $\boxed{-7\ \Delta LB2\quad \Delta M8}$ in our residual renorm. formula.

Residual renormalization formula

The physical contribution from Set V

$$
\begin{aligned}
A_1^{(10)}[\text{Set V}] = \Delta M_{10}[\text{Set V}] \\
&+ \Delta M_8(-7\Delta LB_2) \\
&+ \Delta M_6\{-5\Delta LB_4 + 20(\Delta LB_2)^2\} \\
&+ \Delta M_4\{-3\Delta LB_6 + 24\Delta LB_4\Delta LB_2 - 28(\Delta LB_2)^3 + 2\Delta L_{2^*}\Delta dm_4\} \\
&+ M_2\{-\Delta LB_8 + 8\Delta LB_6\Delta LB_2 - 28\Delta LB_4(\Delta LB_2)^2 \\
&\qquad + 4(\Delta LB_4)^2 + 14(\Delta LB_2)^4 + 2\Delta dm_6\Delta L_{2^*}\} \\
&+ M_2\Delta dm_4(-16\Delta L_{2^*}\Delta LB_2 + \Delta L_{4^*} - 2\Delta L_{2^*}\Delta dm_{2^*}),
\end{aligned}
$$

where quantities w/ Δ are **finite** *n*th-order ones. (*n*=2,4,6,8, and 10)

- *ΔLBn* vertex and wave-function renom. constants.
- *Δdmn* mass-renormalization constants.
- *ΔLn*, Δdmn** * indecates that it has one mass-insertion
- *ΔMn, M2* finite magnetic moments numerically calculated w/ help of gencodeN

We need not to subtract IR divergence from *Ln* and from *Bn*,

when we numerically calculate *ΔLBn*. *Thanks the Ward-Takahashi identity.*

Numerical value of Set V contribution

Substitute the following numbers to the residual renorm. formula:

Integral	Value (Error)	Integral	Value (Error)
ΔM_{10}	3.468 (336)	ΔL_{4^*}	−0.459 051 (62)
ΔM_8	1.738 12 (85)	ΔL_{2^*}	−0.75
ΔM_6	0.425 8135 (30)	Δdm_6	−2.340 815 (55)
ΔM_4	0.030 833 612 $\cdots$	Δdm_4	1.906 3609 (90)
M_2	0.5	Δdm_{2^*}	−0.75
ΔLB_8	2.0504 (86)		
ΔLB_6	0.100 801 (43)		
ΔLB_4	0.027 9171 (61)		
ΔLB_2	0.75		

ΔLB8 and *ΔL4** are newly calculated for Set V. Others are known.

ΔLB8 is the sum of 47 integrals evaluated numerically. The programs are obtained by using the automation gencodeLBn, a slight modification of gencodeN.

We obtain

$$\boxed{A_1^{(10)}[\text{Set V}] = 8.726\ (336).}$$

The uncertainty of the numerical evaluation of *ΔM10* dominates.

Numerical evaluation of *ΔM10*

The shift of the 10^{th}-order term comes from the shift of *ΔM10*.

AHKN, 2014

$$A_1^{(10)}[\text{Set V}] = 8.726\ (336).$$

$$\Delta M_{10}[\text{Set V}] = 3.468\ (336)$$

AHKN, 2012

$$A_1^{(10)}[\text{Old Set V}] = 10.092\ (570).$$

$$\Delta M_{10}[\text{Old Set V}] = 4.877\ (570)$$

shift −1.4

Why it happened?

Uncertainties of each 389 integrals is

less than 0.038

Reliable uncertainty

less than 0.050

Underestimate for some class of integrals

To explain it, let us divide 389 integrals into two classes:

XL 153 diagrams including no self-energy(s.e.) subdiagrams

XB 236 diagrams including at least one s.e. subdiagram.

Numerical properties of *XL* and *XB*

	XL	***XB***
# of integrals	153	236
# of s.e. subdiagrams	0	Ns =1, 2, 3, or 4
dimension of an integral	13	13 − Ns
UV cancelation	Logarithmic	Logarithmic
IR cancelation	None, no IR divergence	Power law divergence
precision required for real numbers	double precision	quadruple precision for some integrals double for rest of integrals

XL is relatively easy to perform numerical integration.

XB is tough due to the *digit-deficiency* problem.

Integration performed so far

performance	# of integrals	dimension	mapping	Precision
XL1	153	13	default	double
XL2	153	13	adjusted	double
XB1	236	13	default	double
XB2a	162	13−Ns	adjusted	quadruple
XB2b	74=236-162	13−Ns	adjusted	quadruple
XB3	176 60	13−Ns	adjusted	double quadruple

Large discrepancy in some integrals are found

b/w *XL1* and *XL2*, and b/w *XB1* and {*XB2* or *XB3*}

XB2 and *XB3* are consistent each other.

The uncertainties of *XL1* and *XB1* are underestimated.

ΔM10[Set V: *2012*] = *XL1 (153)* + *XB2a(162)* + *XB1(74=236-162)*

We excluded the results *XL1* and *XB1* whose mappings are default.

ΔM10[Set V: *2014*] = *XL2 (153)*

+ statistical average of { {*XB2a(162)+XB2b(74)*} & *XB3(236)*}

Mapping of Feynman parameters

Our integrals ***XL*** and ***XB*** are defined w/ 14 Feynman parameters.

Each are assigned to 9 electron lines and 5 photon lines

w/ the constraints:

$$1 = z1 + z2 + z3 + \ldots.. + z8 + z9 + za + zb + \ldots + ze$$

$$0 \leq zi \leq 1, \text{ for } i=1, 2, \ldots, 9, a, b, \ldots, e.$$

The numerical integration algorithm VEGAS uses

a unit hypercube as an integration volume.

There are many ways to map the hyperplane z1+…+ze=1 onto

a 13 dimensional unit cube.

- The result of the integration must not depend on choice of the mapping. → good check of the numerical integration
- Different mappings show different convergent speed of VEGAS.

  There is no 1st principle to pick up the best mapping.

  But, we know by experience what better mappings are.

Mapping example

X001(abacbdcede) from ***XL***

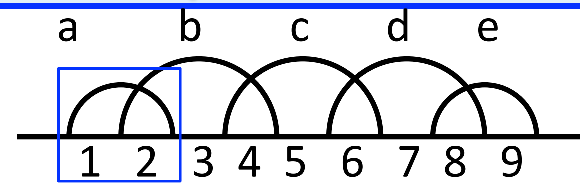

- Mappping in *XL1*

z1a9e=1-q(1), where z1a9e=z1+za+z9+ze

zrest=q(1)

z1a=z1a9e q(2) and so on.

VEGAS output
iteration no.100: integral =-0.0018 ± 0.3567
accumulated results: final value =-0.3398 ±0.0502
chi**2 per it'n = 1.487

UV singularity z12a→0 of $L2^{UV}$ is concentrated in q(2)→0 and q(4)→0 .

- Mapping in *XL2*

z12a34b=q(1)

z12a=z12a34b q(2)

z12=z12a q(3) and so on.

VEGAS output
iteration no.100: integral =-0.1797 ± 0.1268
accumulated results: final value =-0.1748 ±0.0181
chi**2 per it'n = 0.9653

UV singularity z12a→0 of $L2^{UV}$ is translated into q(2) → 0.

VEGAS forms its grid structure looking at

the shape of an integrand projected onto each dimension.

A better grid structure is more rapidly achieved

if the important region of the integral is in the edges of one dimension.

Numerical results of Set V: X001-X099

dgrm	sub.	Value (Error)	it	dgrm	sub.	Value (Error)	it	dgrm	sub.	Value (Error)	it
X001	47	-0.1724(91)	20	**X002**	47	-5.9958(333)	13	**X003**	19	-0.1057(52)	10
X004	71	5.1027(339)	9	**X005**	43	1.1112(168)	20	**X006**	59	-5.2908(245)	9
X007	47	-3.4592(254)	25	**X008**	47	-16.5070(289)	11	**X009**	19	-3.1069(71)	24
X010	83	11.2610(337)	128	**X011**	43	6.0467(338)	22	**X012**	67	-9.3328(267)	26
X013	7	-1.3710(31)	2	**X014**	31	0.8727(42)	10	**X015**	2	2.1090(8)	2
X016	2	-0.9591(7)	2	**X017**	6	0.5146(13)	20	**X018**	6	0.0309(13)	20
X019	31	1.2965(48)	10	**X020**	134	-8.1900(318)	43	**X021**	11	-0.2948(15)	10
X022	79	0.8892(226)	22	**X023**	27	0.4485(55)	25	**X024**	75	-6.0902(246)	23
X025	39	-0.7482(194)	20	**X026**	95	-7.8258(277)	8	**X027**	15	-2.3260(54)	13
X028	71	4.5673(331)	53	**X029**	35	6.9002(233)	1	**X030**	67	-12.6224(328)	38
X031	2	2.3000(14)	4	**X032**	2	-0.2414(6)	2	**X033**	2	-1.3806(7)	2
X034	2	1.2585(9)	4	**X035**	2	-0.5899(3)	2	**X036**	11	0.2318(11)	30
X037	2	-0.7407(5)	2	**X038**	11	-0.2927(14)	20	**X039**	11	0.3292(12)	10
X040	47	1.3397(50)	12	**X041**	63	3.1076(94)	25	**X042**	119	-4.1353(192)	20
X043	15	-2.9620(29)	21	**X044**	59	4.4121(281)	4	**X045**	43	3.4331(212)	20
X046	95	-7.7564(339)	15	**X047**	2	-4.4496(40)	8	**X048**	2	-0.8061(8)	2
X049	2	-0.0278(7)	2	**X050**	2	-1.2213(9)	4	**X051**	2	-0.1776(6)	2
X052	11	1.0293(17)	20	**X053**	2	0.3699(4)	2	**X054**	11	-0.5174(11)	20
X055	2	-0.3673(4)	2	**X056**	11	-0.2650(27)	20	**X057**	23	2.7370(31)	30
X058	44	-5.2510(70)	12	**X059**	23	2.1866(28)	30	**X060**	92	-3.2089(188)	22
X061	68	-3.7724(137)	20	**X062**	161	5.9174(262)	26	**X063**	6	3.4295(14)	20
X064	6	-0.2772(8)	20	**X065**	6	0.1551(13)	20	**X066**	26	-3.6145(45)	21
X067	50	-1.6761(85)	25	**X068**	98	2.7855(217)	22	**X069**	18	-1.2627(31)	11
X070	70	3.2149(144)	20	**X071**	54	3.7025(96)	20	**X072**	134	-5.5704(208)	15
X073	47	3.4114(254)	24	**X074**	47	4.4104(251)	49	**X075**	47	-8.1138(340)	33
X076	19	-5.3405(74)	26	**X077**	39	3.5459(86)	56	**X078**	39	1.1666(80)	56
X079	71	5.3956(305)	41	**X080**	43	0.4597(257)	28	**X081**	59	-5.6566(248)	26
X082	47	-8.5083(339)	97	**X083**	47	18.7498(340)	122	**X084**	19	8.9888(129)	20
X085	39	-2.2833(197)	20	**X086**	39	0.5180(223)	20	**X087**	77	-16.5792(342)	167
X088	43	-5.2606(340)	58	**X089**	63	12.6779(330)	63	**X090**	19	1.5206(130)	20
X091	39	-1.6355(97)	56	**X092**	39	2.1303(218)	15	**X093**	7	-1.7594(42)	10
X094	15	-1.0419(66)	10	**X095**	7	0.5838(35)	6	**X096**	31	1.3458(73)	10
X097	17	5.0319(89)	24	**X098**	33	-1.9806(183)	20	**X099**	39	3.0771(187)	20

Numerical results of Set V: X100-X198

dgrm	sub.	Value (Error)	it	dgrm	sub.	Value (Error)	it	dgrm	sub.	Value (Error)	it
X100	77	-15.2924(314)	248	**X101**	15	-0.2462(64)	12	**X102**	31	-1.2883(75)	26
X103	31	0.9424(74)	10	**X104**	79	6.4131(298)	42	**X105**	35	3.0503(215)	21
X106	71	-11.5662(344)	48	**X107**	43	-4.6643(338)	80	**X108**	63	12.9812(334)	61
X109	17	-0.0860(85)	25	**X110**	35	1.9248(204)	20	**X111**	33	3.3578(132)	24
X112	71	-11.8998(332)	53	**X113**	39	-4.3847(322)	16	**X114**	63	11.0640(336)	58
X115	7	-0.5974(52)	12	**X116**	7	1.8362(28)	10	**X117**	7	0.3292(27)	10
X118	15	-3.2721(55)	10	**X119**	15	-0.0751(53)	10	**X120**	31	1.8769(72)	10
X121	7	-0.8549(43)	6	**X122**	7	-0.7337(42)	6	**X123**	15	-3.3559(67)	12
X124	29	11.5746(106)	26	**X125**	31	0.8677(64)	10	**X126**	59	-1.5696(162)	26
X127	15	1.1412(46)	10	**X128**	31	0.6493(59)	10	**X129**	31	1.4833(70)	10
X130	59	-1.5696(180)	20	**X131**	59	3.1060(287)	33	**X132**	101	-8.8300(337)	43
X133	17	2.7263(88)	24	**X134**	33	-0.6712(123)	23	**X135**	33	0.9256(153)	22
X136	65	-7.5256(305)	46	**X137**	45	-2.3541(233)	23	**X138**	85	10.1610(284)	38
X139	47	14.8674(342)	110	**X140**	39	-2.7901(206)	21	**X141**	74	-12.5546(342)	271
X142	43	-1.5792(339)	67	**X143**	61	10.3213(335)	61	**X144**	83	23.7226(360)	241
X145	67	-18.6193(338)	122	**X146**	39	-2.2990(335)	25	**X147**	15	1.1243(55)	20
X148	31	-1.4150(76)	21	**X149**	17	-8.3898(139)	19	**X150**	33	2.8758(260)	2
X151	87	-10.9356(335)	72	**X152**	77	14.6695(335)	119	**X153**	77	14.8910(335)	84
X154	67	-20.6259(334)	94	**X155**	15	5.0341(46)	20	**X156**	31	-0.8277(69)	14
X157	32	-11.8490(252)	18	**X158**	65	0.4607(329)	6	**X159**	65	0.4435(351)	27
X160	116	14.0722(345)	182	**X161**	71	7.8089(336)	71	**X162**	95	-12.8293(339)	43
X163	19	6.8168(202)	21	**X164**	19	-12.8880(208)	3	**X165**	15	-2.1661(76)	10
X166	15	-2.3080(70)	10	**X167**	29	12.1361(150)	20	**X168**	17	3.4447(120)	24
X169	25	-6.9379(108)	20	**X170**	39	0.2635(288)	36	**X171**	39	-2.5229(313)	7
X172	31	1.5601(76)	26	**X173**	59	0.0193(298)	48	**X174**	35	1.7158(191)	25
X175	51	-1.8253(175)	19	**X176**	7	0.7450(35)	20	**X177**	15	0.0079(81)	21
X178	5	0.7159(28)	2	**X179**	2	-0.4377(8)	4	**X180**	11	0.0284(25)	4
X181	6	-4.4372(28)	30	**X182**	12	1.2822(43)	20	**X183**	7	-0.0791(29)	20
X184	31	0.1973(134)	25	**X185**	5	-0.1269(16)	10	**X186**	23	1.1883(21)	10
X187	6	1.2699(27)	20	**X188**	24	1.7966(36)	11	**X189**	17	-3.7500(105)	20
X190	33	-2.4966(217)	20	**X191**	13	0.1892(62)	11	**X192**	25	2.3868(91)	24
X193	15	-4.2570(84)	19	**X194**	27	-0.6785(102)	25	**X195**	2	-1.0708(19)	10
X196	2	-2.0432(20)	6	**X197**	2	-0.3848(8)	2	**X198**	5	-2.3533(26)	2

Numerical results of Set V: X199-X297

dgrm	sub.	Value (Error)	it	dgrm	sub.	Value (Error)	it	dgrm	sub.	Value (Error)	it
X199	5	1.0636(26)	2	**X200**	11	0.0266(26)	4	**X201**	2	-0.4897(18)	6
X202	2	1.9313(17)	6	**X203**	2	0.9061(10)	4	**X204**	11	-1.9485(26)	2
X205	5	-0.9039(13)	10	**X206**	23	1.6836(23)	10	**X207**	5	0.2908(23)	2
X208	11	0.5283(28)	2	**X209**	5	0.1496(19)	2	**X210**	23	0.7803(19)	10
X211	23	5.1339(90)	12	**X212**	41	-0.4617(138)	25	**X213**	6	-2.4516(29)	20
X214	12	0.6801(39)	20	**X215**	6	0.0724(24)	20	**X216**	24	-1.3029(42)	12
X217	18	-2.2261(71)	15	**X218**	30	-1.6396(84)	25	**X219**	39	1.3579(311)	5
X220	59	-2.5734(222)	27	**X221**	35	0.6650(161)	20	**X222**	51	0.8293(178)	20
X223	116	17.5190(339)	135	**X224**	31	2.4729(110)	20	**X225**	23	0.3434(39)	10
X226	13	1.0443(58)	11	**X227**	25	0.5835(97)	21	**X228**	75	-6.8113(333)	52
X229	35	-1.9843(323)	11	**X230**	71	15.6790(342)	121	**X231**	11	-0.7737(28)	10
X232	23	0.4608(38)	10	**X233**	31	8.6698(116)	25	**X234**	63	-2.5793(179)	21
X235	23	0.7486(35)	10	**X236**	63	2.0560(180)	20	**X237**	113	-12.9913(363)	154
X238	25	1.2747(45)	21	**X239**	69	-2.8075(345)	49	**X240**	93	10.9428(298)	55
X241	43	13.8127(349)	140	**X242**	68	-10.4867(377)	183	**X243**	57	3.8891(336)	44
X244	35	-3.3041(334)	10	**X245**	27	0.0658(83)	12	**X246**	29	-0.3959(174)	20
X247	39	15.9592(335)	46	**X248**	31	-1.9165(278)	2	**X249**	13	4.0116(46)	20
X250	27	-1.0558(68)	24	**X251**	27	-1.3906(76)	12	**X252**	56	-10.9021(335)	34
X253	113	17.8455(345)	231	**X254**	29	2.2265(175)	20	**X255**	43	8.1598(340)	6
X256	93	-14.0423(340)	82	**X257**	7	5.7475(51)	11	**X258**	7	-0.5254(39)	20
X259	5	0.0053(27)	10	**X260**	5	-0.3958(20)	2	**X261**	6	6.4046(30)	20
X262	6	-2.2854(24)	20	**X263**	7	-2.8330(35)	20	**X264**	15	4.8826(64)	12
X265	5	-0.6756(20)	2	**X266**	11	0.1206(23)	10	**X267**	6	-0.6608(19)	20
X268	12	0.1185(31)	20	**X269**	15	-0.7190(56)	12	**X270**	31	-1.6881(97)	25
X271	11	0.2492(23)	10	**X272**	23	-0.7285(32)	10	**X273**	13	-2.0474(45)	11
X274	25	0.8675(72)	24	**X275**	2	-0.7496(12)	10	**X276**	2	-0.5547(10)	4
X277	2	2.7936(10)	4	**X278**	5	-0.1577(23)	10	**X279**	5	0.8399(15)	2
X280	2	-1.0127(8)	10	**X281**	5	-1.3732(25)	2	**X282**	5	0.4907(18)	2
X283	11	-0.0427(23)	2	**X284**	2	-0.2670(9)	2	**X285**	5	0.0271(16)	2
X286	11	0.8014(21)	2	**X287**	23	0.2013(19)	10	**X288**	6	4.2112(28)	20
X289	6	-1.5651(19)	20	**X290**	6	-3.7763(23)	20	**X291**	12	1.5957(32)	20
X292	12	0.9114(36)	20	**X293**	24	-1.2653(41)	11	**X294**	7	-3.3891(25)	20
X295	7	1.7883(26)	20	**X296**	5	0.5511(13)	10	**X297**	5	-0.4696(16)	10

Numerical results of Set V: X298-X389

dgrm	sub.	Value (Error)	it	dgrm	sub.	Value (Error)	it	dgrm	sub.	Value (Error)	it
X298	6	-1.9142(28)	20	**X299**	6	-0.2907(22)	20	**X300**	29	-9.4327(194)	28
X301	31	-1.3351(81)	22	**X302**	59	-1.8294(223)	30	**X303**	2	0.3341(7)	2
X304	5	-0.3397(16)	10	**X305**	5	0.4715(14)	2	**X306**	23	0.1228(55)	20
X307	47	-0.3071(59)	21	**X308**	6	1.8122(22)	20	**X309**	26	-4.2448(173)	20
X310	50	0.2490(191)	21	**X311**	15	-0.5291(58)	12	**X312**	31	-1.2454(139)	14
X313	11	0.9660(38)	4	**X314**	23	0.8266(29)	10	**X315**	13	-1.3728(43)	20
X316	25	0.0094(39)	12	**X317**	59	1.4535(221)	23	**X318**	62	-8.7599(340)	60
X319	47	0.6801(179)	25	**X320**	11	0.5627(17)	10	**X321**	23	-0.9005(26)	10
X322	23	0.9338(23)	2	**X323**	25	-0.0053(40)	12	**X324**	53	-8.8058(243)	23
X325	107	11.5958(343)	51	**X326**	17	-9.0047(145)	24	**X327**	33	1.5517(229)	29
X328	13	-0.2781(42)	20	**X329**	25	-0.9627(67)	11	**X330**	15	-4.9591(88)	14
X331	27	4.7241(127)	25	**X332**	33	3.0539(161)	25	**X333**	65	6.8060(331)	52
X334	47	5.1727(340)	23	**X335**	37	-2.0294(132)	25	**X336**	6	-0.7685(20)	20
X337	12	-1.2039(32)	20	**X338**	13	-1.8505(38)	20	**X339**	25	0.4111(40)	12
X340	53	-2.1543(202)	25	**X341**	24	1.7815(33)	20	**X342**	27	2.6063(125)	0
X343	2	3.8873(30)	6	**X344**	2	3.4223(18)	6	**X345**	2	-1.0075(18)	4
X346	2	0.2864(20)	6	**X347**	2	-2.6846(21)	6	**X348**	2	-0.4899(15)	4
X349	5	2.0800(36)	2	**X350**	2	1.4643(11)	4	**X351**	5	0.2554(20)	2
X352	2	-0.1260(8)	2	**X353**	5	0.1950(16)	2	**X354**	5	-2.0503(20)	2
X355	11	-1.0738(25)	2	**X356**	5	2.0684(24)	10	**X357**	5	0.3746(16)	2
X358	5	0.0463(16)	2	**X359**	11	-0.1396(17)	10	**X360**	11	-0.4604(37)	2
X361	23	2.5600(26)	10	**X362**	2	-0.5714(12)	4	**X363**	2	-2.3442(19)	4
X364	2	2.3957(18)	4	**X365**	11	0.4177(30)	20	**X366**	23	5.6759(43)	20
X367	5	-0.7176(12)	10	**X368**	23	-0.3404(45)	20	**X369**	47	-3.3812(59)	21
X370	5	-1.4763(12)	10	**X371**	5	0.0045(10)	2	**X372**	11	-1.2900(33)	2
X373	23	0.5851(24)	2	**X374**	47	0.9188(266)	18	**X375**	89	1.0991(163)	25
X376	5	1.0484(16)	2	**X377**	11	0.4264(27)	2	**X378**	11	1.3196(21)	2
X379	23	-0.3201(17)	10	**X380**	47	-1.0268(48)	21	**X381**	23	1.0861(29)	2
X382	41	-1.7712(80)	21	**X383**	6	-4.8034(22)	20	**X384**	12	1.9266(31)	20
X385	12	-0.7427(19)	20	**X386**	24	0.6887(38)	11	**X387**	50	1.9508(152)	21
X388	24	-0.4349(40)	20	**X389**	30	-0.0433(68)	25				

Conclusion

The updated QED value of the electron *g-2* leads to a new value of the fine-structure constant:

$$\alpha^{-1}(a_e : \mathrm{HV08}\ \&\ \mathrm{QED14}) = 137.035\ 999\ 1570\ (29)(27)(18)(331)\ [0.25\mathrm{ppb}]$$

QED 8th, 10th , Weak&Hadron, Experiment

1. The goal of QED calculation is to reduce the uncertainty of QED term smaller than that of the Weak & Hadronic term.
2. We are very sure that there are no analytic errors in our 8th- and 10th-order QED calculations.
3. Improvement of the 8th and 10th-order terms relies on future numerical work.

- A new Vegas (2013) by P. Lepage has more refined algorithm for a grid formation. Maybe helpful. https://github.com/gplepage/vegas
- RIKEN RICC was shutdown at the end of 2014.

  An entirely new machine will launch in April of 2015. Maybe helpful, too.

Values of the fine-structure constant

$$\left[\alpha^{-1} - 137.035999\right] \times 10^{9}$$

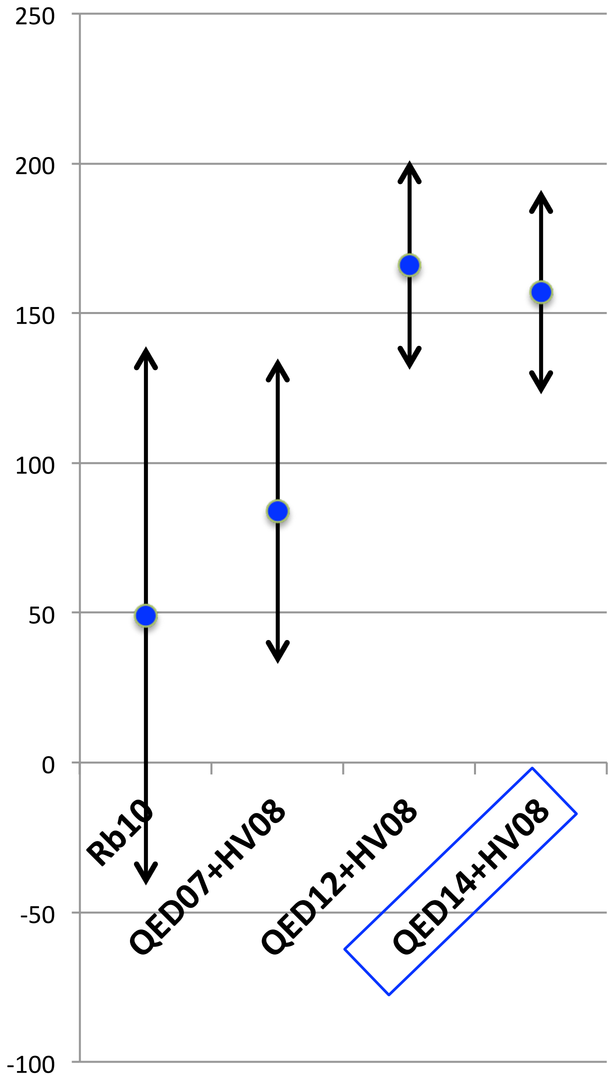

Thank you